

Morphologic reproducibility in 6 regions of the 3-dimensional facial models acquired by a standardized procedure: An in vivo study

Xin-wen Wang,^a Zi-jin Liu,^a Jing Diao,^b Yi-jiao Zhao,^c and Jiu-hui Jiang^a
Beijing, China

Introduction: A standardized procedure was proposed to control involuntary motion and other factors during the capture of structural light scanning that could influence the morphology of 3-dimensional facial models; interoperator reproducibility was evaluated. **Methods:** Twenty subjects volunteered for facial scanning. Three researchers scanned each volunteer 3 times on the same day using the FaceScan structural light scanning system (Isravision, Darmstadt, Germany) and after the proposed procedure. Captures were done at 5-minute intervals. The 3 facial scans acquired by the same researcher were compared by reverse engineering software (Geomagic; 3D Systems, Rock Hill, SC). Six facial regions, including forehead, nose, paranasal, upper lip, lower lip and chin, and cheek, were divided. With the first scan as a reference, the other 2 scans were registered, and surface-to-surface distance maps were acquired to calculate the mean, standard deviation, and root mean squares (RMS) between 2 surfaces. The reproducibility between 3 researchers was then evaluated by a 1-way analysis of variance. **Results:** The mean of 6 facial regions was close to 0. The RMS of lip regions were largest (0.48-0.53 mm), the forehead was smallest (0.21 mm), and the others ranged 0.37 mm to 0.42 mm. The standard deviation was slightly smaller than RMS and had the same trend of change. There was no significant difference in RMS among the 3 researchers ($P > 0.05$). **Conclusions:** With the constraint of the standardized procedure, the morphologic reproducibility of facial models in 6 regions was satisfying. (Am J Orthod Dentofacial Orthop 2022;161:e287-e295)

Changes in facial morphology are of great concern in orthodontics and dentofacial orthopedics. For recording facial morphology, 3-dimensional (3D) facial models are superior to 2-dimensional photographs. Structural light scanning (SLS) is a 3D facial recording method that reproduces the shape, color, and texture of the human face in the OBJ file format.

In most research, 3D facial models are still measured in length and angle.¹⁻¹⁰ It has been shown that the SLS system demonstrated high accuracy, reliability, and reproducibility^{2,3,11-14} in linear and angular measurements. The nominal accuracy of the FaceScan (Isravision, Darmstadt, Germany) SLS system is 0.2 mm, and practical accuracies for length and angle measurement were -0.29 ± 0.53 mm and $0.12^\circ \pm 2.69^\circ$, respectively.³ However, linear and angular measurements fail to take full advantage of a huge amount of information recorded. Facial volume measurement was first proposed in 1954,¹⁵ and is widely used in the field of orthognathic,¹⁶⁻¹⁹ rejuvenation surgery,²⁰ facial growth,^{21,22} infantile hemangioma,²³ cleft lip deformity,²⁴ and other circumstances in which facial volume change.^{25,26} Nowadays, it has become more and more popular to register 2 different 3D scans, generate surface-to-surface distance maps to demonstrate possible change. The volume measurement and the distance maps have 2 problems: (1) the reproducibility of facial model morphology has scarcely been studied. Thus no one can

^aDepartment of Orthodontics, Peking University School and Hospital of Stomatology, Beijing, China.

^bDepartment of Preventive Medicine, Peking University School and Hospital of Stomatology, Beijing, China.

^cNational Engineering Laboratory for Digital and Material Technology of Stomatology, Beijing, China.

All authors have completed and submitted the ICMJE Form for Disclosure of Potential Conflicts of Interest, and none were reported.

Address correspondence to: Jiu-hui Jiang, Department of Orthodontics, Peking University School and Hospital of Stomatology, No. 22 Zhongguancun South Ave, Haidian District, Beijing, China 100081; e-mail, drjiangw@163.com.

Submitted, August 2020; revised and accepted, November 2020.

0889-5406/\$36.00

© 2021 by the American Association of Orthodontists. All rights reserved.

<https://doi.org/10.1016/j.ajodo.2020.11.042>

tell how minimum volume change can be detected by SLS; (2) the definition of facial region is vague and different studies have different regions proposed.

Secher et al¹³ found that head position, facial expression, mandibular position, occlusion, and forehead exposure (relating to registration) may influence facial morphologic reproducibility in SLS. Rawlani et al²⁵ also found that subtle facial expressions may result in apparent volumetric alterations in the mid and lower face. In 2019, there is a systematic review and meta-analysis for the reliability of optical devices for 3D facial anatomy description, which concluded that for surface-to-surface measurements, the fast device should be preferred, and dedicated protocols devised to avoid motion artifacts.¹⁴

To reduce the error during the SLS capture, a new standard procedure was developed to control head position, facial expression, mandible position, occlusion, forehead exposure, and other instrumental factors. A new method to divide the face into 6 regions was also proposed: the forehead, nose, paranasal area (left and right), cheek (left and right), upper lip, and lower lip and chin.

The purpose of this study was to establish a standardized procedure to acquire highly reproducible 3D facial models for a real person and test the reproducibility in 6 facial regions.

MATERIAL AND METHODS

Twenty volunteers were recruited from Peking University School of Stomatology. Inclusion criteria were aged 18–30 years with a balanced face. Exclusion criteria were obvious facial deviation (>3 mm chin deviation, asymmetry of bilateral buccal soft tissues), severe skeletal Class II and III malocclusion, congenital facial deformity (such as cleft lip and palate). This study was approved by the ethics committee of Peking University School of Stomatology, Beijing, China (no. PKUSSIRB-201942005). Informed consent was obtained from all volunteers in writing.

Three researchers (X.W, Z.L, and J.D) individually captured SLS (FaceScan) 3 times for each volunteer. Each capture was 5 minutes apart, and the scan time was 0.8 seconds. During the interval, the subject can talk and walk outside to simulate different visits. The order of the 3 researchers was randomly decided by the stochastic indicator.

In the proposed procedure, the materials and tools are listed as follows (Fig. 1): (1) SLS machine (FaceScan); (2) height-adjustable round stool, with a height range of 48–68 cm; (3) 2-plane leveling and alignment lasers (GCL2-15G; Bosch, Gerlingen, Germany); and (4) 2-



Fig 1. The 2-plane leveling and alignment lasers and the fixing and adjusting devices: **A**, orthogonal laser; **B**, 2-way focusing adjuster; **C**, customized connectors; **D**, the pole of SLS machine; **1**, up and down adjustment knob; **2**, left and right adjustment knob.

way focusing adjuster (Velbon Super Mag Slider) and customized connectors (to fasten the 2-way focusing adjuster and the alignment lasers to the pole of the SLS machine).

During each capture, the standardized procedure was followed: (1) inform the subject that we will take a 3D photograph and let the subject know what will be expected of them later; train the subject's natural head position, jaw rest position, and neutral expression¹³ several times; (2) make sure the whole forehead is exposed; (3) adjust the seat height to ensure the head is within the exposure coverage of the machine. The forward-backward and left-right position of the seat was fixed in advance (Fig. 2), which was the same for all subjects; (4) adjust the mirror behind the subject bilaterally to make its bracket foot conform to the predetermined mark on the ground (Fig. 2). This step makes sure the SLS machine works in the same condition; (5) ask the volunteer to sit upright with both hands on the thighs, look straight ahead, with their head in a comfortable and balanced position (Fig. 2). Then, tell the subject to close their eyes. Adjust the head position into estimated natural head position (eNHP)²⁷ with an orthogonal laser; (6) tell the subject to open their eyes, look straight ahead, and wear neutral expression²⁵ with mandible at a relaxed

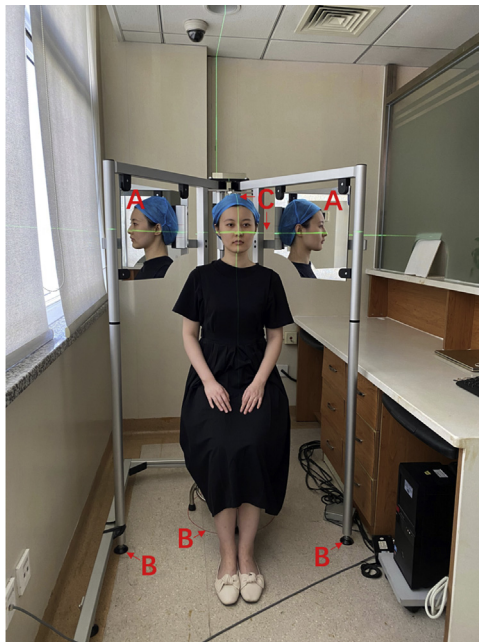


Fig 2. A patient positioned for standardized image acquisition: **A**, bilateral mirrors in which yaw angle of the head can be observed; **B**, predetermined mark on the ground to regulate the position of the round stool and the bracket foot of the mirrors; **C**, orthogonal lasers projected onto the patient's face, note the vertical laser passes through the midsagittal plane, whereas the horizontal laser passes between infraorbital margin and nose tip.

position; (7) press the shutter, check the completeness of the scan (especially the lower margin of the mandible, the nose tip, the lip commissure, and the tragus), and export in the OBJ file format. The researcher's gaze should pass through the center of the subject's face and be perpendicular to it all the time; the wrong viewing angle will lead to misjudgment of eNHP.

The standard of eNHP was studied by the 3 researchers previously, who had assessed 20 pairs of frontal and lateral photographs individually and wrote down how the subject's head deviates from natural head position (NHP), using "pitch down, pitch up, roll left, roll right, yaw left, yaw right" in the description. Then, the opinions about the head position were checked, discussed, and corrected until a consensus about eNHP was reached. In the standard procedure, the subjects' head was adjusted to eNHP, meeting the accepted standards.

With the autocalibration function, the orthogonal laser emits a horizontal laser parallel to the ground plane and a vertical laser perpendicular to it. The lasers projected onto the face were not only a frame of reference to evaluate the head position but also a record of the world coordinate system. To avoid potential harm to

the eyes, the eyes should be closed before the laser to be adjusted to the ideal position, in which the vertical laser passes through the midsagittal plane, whereas the horizontal laser passes between the infraorbital margin and nose tip (Fig. 2). The laser height and left-right position were adjustable by the 2-way focusing adjuster.

The 3 different scans shot by the same researcher were processed by the Geomagic 2014 (2014, Germany) software (3D Systems, Rock Hill, SC). The process flow was as follows:

1. Alignment and registration: the first model was set to the fixed module, whereas the second and third models were floating modules to match the first model. The 3 different facial models were aligned preliminarily on the basis of 6 landmarks (bilateral endocanthion, bilateral exocanthion, and postero-tragion; Table 1, Fig. 3). Because the forehead remains relatively fixed with facial animations,²⁵ it was chosen for matching different scans by iterative closest point algorithm, which was also called registration. How to define the forehead boundary will be discussed later. This step realizes the superimposition of 3 different facial models.
2. Facial region division (Fig. 3): the facial region was divided into 2 types of boundaries, including the boundary with clear landmarks or boundary with no clear landmarks (BNCL). The boundary with clear landmarks was obtained by the draw operation: locate 2 end points and automatically draw an arc on the model with the shortest distance between the 2 landmarks. BNCL was used for 2 conditions: (1) the area between 2 points was unsmooth, such as the lower border of the upper lip and the upper border of the lower lip; and (2) no clear landmarks were included, such as the lower border of the mandible and the upper border of the forehead. Any number of points can be used in BNCL to make it conform to the shape of the actual model as much as possible. BNCL was subjective and should be checked 3-dimensionally.

The landmarks used in the proposed method are in Table 1.

As a result, 6 regions were acquired in 1 of the 3 facial models (Fig. 3), and they should be the same as the other 2 models as far as possible. The project function was used to copy boundaries in different models, especially useful in the smooth area without clear landmarks. The whole boundaries of the forehead and the lower border of the mandible were copied by the project function, whereas the other borders were obtained in the same way introduced earlier.

Table I. Abbreviations and definitions of landmarks used in the study

Landmark	Abbreviations	Definition
Endocanthion	en'	Most medial point of the palpebral fissure, at the inner commissure of the eye; best seen when the subject is gazing upward
Exocanthion	ex'	Most lateral point of the palpebral fissure, at the outer commissure of the eye; best seen when the subject is gazing upward
Posterotragion	pt'	The most posterior point on the tragus
Sellion	se'	Deepest midline point of the nasofrontal angle
Parasellion*	ps'	The most concave point between the se' and en'
Ciliare lateralis	cl'	The most lateral peak and extent of the eyebrow
Ciliare medialis	cm'	The most medial and inferior corner of the eyebrow (not present when the eyebrows cross glabella)
Subnasale	sn'	The median point at the junction between the lower border of the nasal septum and the philtrum area
Subalare	sbal'	The inferior point at the junction of each nasal alar base with the philtrum area
Alar curvature point	ac'	The most posterolateral point of the curvature of the baseline of each nasal ala
Alare	al'	The most lateral point on the nasal ala
Cheilion	ch'	Outer corners of the mouth where the outer edges of the upper and lower vermilions meet
Chin foot point*	cf'	Through ch' draw a line perpendicular to the lower border of mandible; The intersection point is cf'
Gnathion	gn'	The median point halfway between pg' and me' pg': Most anterior midpoint of the chin, located on the skin surface anterior to the identical bony landmark of the mandible me': Most inferior median point of the chin
Gonion	go'	The most lateral point on the mandibular angle, adjacent to go, identified by palpation
Paranasal point*	pnal'	The intersection point of connection of al'-pt' and ex'-ch'

Note. Landmarks were positioned assuming the FH position. The upper corner maker (') refers to capulometric landmarks (on soft tissue) apart from craniometric landmarks (on the skull).

*Defined by authors; the other points refer to Caple and Stephan.⁴²

3. Facial deviation analysis: each of the 6 regions can be chosen individually to calculate the deviation of any 2 different facial models through the deviation and 3D compare function, Figure 4. The 6 regions make up the whole face. Mean (μ), standard deviation (SD), and root mean square (RMS) were adopted to measure the morphologic deviation of different models in different regions; μ is the mean value of the distance (X_i) between the corresponding points (no. of points is N) of 2 different models, which can be positive, negative, or zero. The definition of SD and RMS were as follows:

$$SD = \sqrt{\frac{1}{N} \sum_{i=1}^N (X_i - \mu)^2}$$

$$RMS = \sqrt{\frac{1}{N} \sum_{i=1}^N X_i^2}$$

Statistical methods

Facial scans of 19 subjects were analyzed, whereas 1 subject was excluded because of obvious face cover. Each subject had 9 scans, acquired by 3 investigators.

Three scans by 1 investigator were processed in Geomagic 2014 software simultaneously to get 3 sets of data (μ , SD, and RMS). Each scan was divided into 6 regions: forehead, nose, paranasal, upper lip, lower lip and chin, cheek, and add up to the whole face. Therefore, for each facial region, there were 171 sets of data, and 7 regions come up to 1197 sets of data. SPSS statistical software (version 23.0; IBM, Armonk, NY) was used for descriptive statistics and verified reliability by 1-way analysis of variance.

RESULTS

Forty extremes for RMS (40 out of 1197) were found by boxplot: 4 in the forehead (4 out of 171), 10 in the nose (10 out of 171), 6 in the paranasal region (6 out of 171), 6 in the upper lip (6 out of 171), 8 in the lower lip and chin (8 out of 171), 2 in the cheek (2 out of 171) and 4 in the whole face (4 out of 171). These extremes were excluded. The study focused on the measurement error of different facial regions during capture and processed the scans under normal conditions. The 40 extremes might occur in the condition that scans defects and bad forehead registration outcome, which was not within consideration.

The descriptive statistics of μ , SD, and RMS are in Tables II-IV. According to Table II, it can be found that the mean values of μ were very close to 0 for the 7

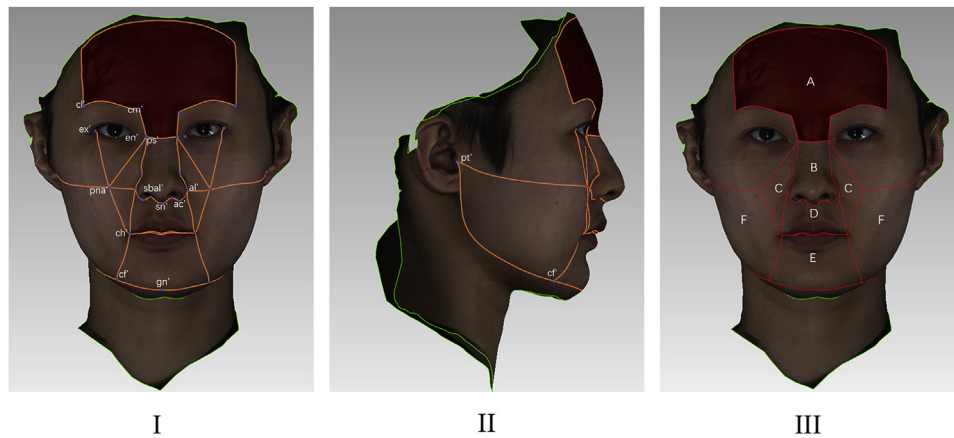


Fig 3. The landmarks used and facial region division. Pictures I and II show the landmarks used in the study. Picture III shows the 6 facial regions: **A**, forehead; **B**, nose; **C**, paranasal region (bilateral); **D**, upper lip; **E**, lower lip and chin; **F**, cheek (bilateral). The orange in pictures I and II are curves, whereas the red in picture III are boundaries. The erase of useless curves and the convert into boundaries are realized in Geomagic (3D Systems, Rock Hill, SC).

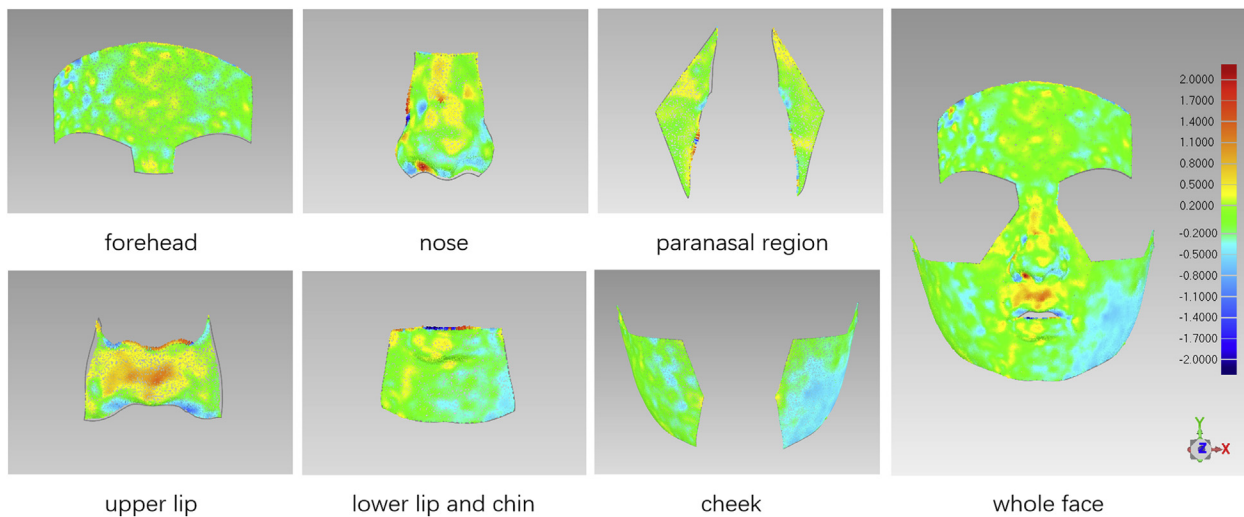


Fig 4. Facial deviation analysis in 6 facial regions and the whole face.

regions, which shows that the mean value of the distance difference between the corresponding points in the 2 different facial models was about 0. SD represents the discrete trend of the distance difference between the corresponding points on 2 different facial models. According to the formula, SD and μ jointly determine the RMS. Because μ was close to 0 and can be positive or negative, RMS was slightly greater than SD. Therefore, RMS can better reflect the deviation of corresponding points in 2 different facial model regions.

Because the registration was based on the forehead, its RMS was the smallest (0.2141 mm; Table IV). It is

worth noting that the RMS of the forehead was not close to 0, indicating that even if it was considered a stable area and matched by iterative closest point algorithm,^{28,29} it still has certain deviation because of structural light imaging quality, subject's expression, and other factors. The RMS of the lower lip and chin (0.5345 mm) was the largest, after the RMS of the upper lip (0.4771 mm), which may be related to the deviation of mandible position and expression of the lip. The lower lip and chin were the farthest from the forehead area may be another possible reason for its large deviation.

Table II. Descriptive statistics of μ in 6 facial regions plus the whole face (in mm)

Region	Mean \pm SD	95% CI
Forehead	-0.0020 \pm 0.0124	-0.0039 to -0.0001
Nose	0.0085 \pm 0.1276	-0.0114 to 0.0283
Paranasal region	0.0071 \pm 0.2233	-0.0273 to 0.0414
Upper lip	-0.0339 \pm 0.2764	-0.0764 to 0.0086
Lower lip and chin	0.0140 \pm 0.3564	-0.0412 to 0.0691
Cheek	-0.0021 \pm 0.1953	-0.0318 to 0.0275
Whole face	0.0008 \pm 0.1238	-0.0181 to 0.0198

Table III. Descriptive statistics of SD in 6 facial regions plus the whole face (in mm)

Region	Mean \pm SD	95% CI
Forehead	0.2112 \pm 0.0464	0.2041-0.2183
Nose	0.3932 \pm 0.0927	0.3788-0.4076
Paranasal region	0.3077 \pm 0.0756	0.2960-0.3193
Upper lip	0.4012 \pm 0.1167	0.3832-0.4191
Lower lip and chin	0.4177 \pm 0.1544	0.3938-0.4416
Cheek	0.3743 \pm 0.1477	0.3519-0.3967
Whole face	0.3726 \pm 0.0980	0.3576-0.3876

Table IV. Descriptive statistics of RMS in 6 facial regions plus the whole face

Region	Mean \pm SD	95% CI
Forehead	0.2141 \pm 0.0329	0.2090-0.2191
Nose	0.4119 \pm 0.0991	0.3964-0.4273
Paranasal region	0.3728 \pm 0.1049	0.3567-0.3890
Upper lip	0.4771 \pm 0.1548	0.4533-0.5008
Lower lip and chin	0.5345 \pm 0.1981	0.5038-0.5651
Cheek	0.4195 \pm 0.1545	0.3960-0.4429
Whole face	0.3906 \pm 0.1051	0.3745-0.4066

The reproducibility among the 3 researchers was evaluated by a 1-way analysis of variance, and the results were shown in Table V. The *P* value of the 7 facial regions were all >0.05 , indicating that there was no statistical difference in the scans of the 3 researchers.

DISCUSSION

A standardized procedure to raise the reproducibility of facial scans in a live subject was proposed in this study. This study adopted a surface-to-surface distance map to calculate 3D error instead of linear and angular measurements in tradition, which provided a reference for future facial volume measurements. The reproducibility was assessed by 6 facial regions of interest in the field of orthodontics and orthognathic. The procedure to divide the 6 regions was proposed and described clearly in this study.

Table V. One-way analysis of variance comparing the RMS of 3 researchers

Region	F	<i>P</i> value
Forehead	1.52	0.22
Nose	1.73	0.18
Paranasal region	0.44	0.64
Upper lip	0.35	0.70
Lower lip and chin	1.14	0.32
Cheek	0.09	0.91
Whole face	0.46	0.63

Several studies also adopted surface-to-surface distance maps to evaluate the reproducibility of 3D facial scanners. Kau et al³⁰ had evaluated the reproducibility of Minolta Vivid 900 laser-scanning devices in 40 subjects. It suggested the mean shell deviations in the superimposition of whole faces were 0.31 ± 0.08 mm for scans taken 3 minutes later and 0.40 ± 0.11 mm for scans 3 days later. The result was similar to 0.39 ± 0.11 mm (RMS for the whole face) in this study. However, the reported manufacturing accuracy of Minolta Vivid 900 was 0.1 mm, which was smaller than FaceScan (0.2 mm) in this study. Secher et al¹³ verified the reproducibility of the DAVID SLS-2 scanner in 10 adults, each scanned twice. The result was that SD values range from 0.3 mm in the eyes; 0.3-0.35 mm in the forehead and nose; 0.5-0.6 mm in the mouth, cheek and chin region; and >2 mm in the neck region. Compared with the current study—in addition to the SD value in the nose region (0.34 mm) slightly smaller than in this study (0.39 mm)—SD values in the other corresponding regions were greater, proving the proposed standardized procedure was effective. Maués et al³¹ studied the reproducibility of a low-cost Microsoft Kinect Scanner in 10 patients; for 10 anatomic facial regions of interest, the SD ranged 0.31 mm to 1.10 mm, which was greater than the results of this study. Gibelli et al³² studied the reproducibility of a low-cost Sense Scanner in 50 adults; the RMS for the whole face was 0.42 ± 0.17 mm by intradevice comparison, which was greater than 0.39 ± 0.11 mm in this study.

In addition, the studies mentioned above, other studies were focused on verifying the practical accuracy of new facial scan devices by comparison with the golden standard. Camison³³ compared Vectra H1 handheld 3D photogrammetry system with validated 3dMD stereophotogrammetry system in 26 adults. The average RMS value of 26 surface-to-surface comparisons was 0.43 mm for the whole face (range, 0.33-0.59 mm). Gibelli et al³⁴ compared portable Vectra H1 with static Vectra M3 devices in 50 adults; each had 4 facial scans (2 for each instrument). The RMS values

for the whole face were 0.22 ± 0.14 mm, 0.44 ± 0.36 mm, and 0.52 ± 0.14 mm for M3-M3, H1-H1, and M3-H1, respectively. Zhao et al³⁵ compared FaceScan and 3dMD with a high-accuracy line-laser scanner (Faro) in 10 patients; each had 3 facial scans. The respective RMS for the whole face of FaceScan and 3dMD was 0.57 ± 0.07 mm and 0.58 ± 0.11 mm. Knoops et al³⁶ had 8 adults acquired facial scans using 4 3D scanners: relative to the 3dMD, accuracy was the highest for M4D Scan (90% within 2 mm; RMS of 0.71 ± 0.28 mm), followed by Avanto magnetic resonance imaging (86%; 1.11 ± 0.33 mm) and structure sensor (80%; 1.33 ± 0.46 mm). Although the results were mostly based on the surface-to-surface comparison of different devices, as long as a real person was captured, the results cannot eliminate the influence of involuntary motion. Therefore, they still had some reference significance. In this study, the RMS of the whole face was 0.39 ± 0.11 mm, with a 95% confidence interval [CI] of 0.37-0.41 mm, which was similar to studies by Camison et al³³ and Gibelli et al,³⁴ whereas smaller than studies by Zhao et al³⁵ and Knoops et al.³⁶

The 95% CI of RMS can provide a reference for minimum detectable facial volume change in future research. For example, the 95% CI of the cheek was 0.3960-0.4429 mm. If the RMS of the cheek was within the range of 0.3960-0.4429 mm before and after treatment, it suggests no volume change of buccal soft tissue. The observed change could be considered beyond measurement error if RMS was greater than the upper limit of 95% CI.

The limitations of forehead registration may be the important reason for the 40 extremes of RMS. The forehead was believed stable and widely used as a registration area in previous studies.³⁷ If there was a distinct inconsistency between the forehead area of 2 facial models, they could not overlap perfectly. The possible reasons for forehead registration failure were (1) the imaging quality of structured light scanning was limited, and thus, deformation of forehead occurs; (2) it was difficult to achieve absolute neutral expression; (3) the proportion of forehead was relatively small for some people; according to the results, 26 of the 40 extreme points appear in people with the small forehead. Therefore, the improvement strategies were (1) control factors that affect the imaging quality, such as ambient light; (2) train the subjects to achieve neutral expression and check the subjects' expression before pressing the shutter; and (3) expand the registration area as much as possible.

Rest jaw position³⁸ was adopted in this study, maintained by passive visco-elastic forces in perioral soft

tissues rather than postural stretch reflexes.³⁹ Thus, the buccal soft tissue volume was not influenced by the contraction of the masticatory muscle. However, the rest jaw position does not define the lip closure or not, which may be an important reason for the largest RMS of the lip regions. Lip contact position was developed by Watarai et al,⁴⁰ placing the mandible in a physiological rest position. It demonstrated excellent reproducibility compared with the rest jaw position. Another benefit was, if the lips were closed, the lower border of the upper lip and the upper border of the lower lip would be simplified into 1 line. It was advised that "jaw relaxation, no occlusion, and lip closure" should be emphasized during instruction.

The repeatability of eNHP was proved to be higher than that of registered natural head position (including self-balanced NHP and mirror method).⁴¹ Limited to the design of FaceScan structural light scanner, the subject's head needs to lean on the head bracket at the back of the instrument during capture. Otherwise, the nose tip may be incomplete on the 3D facial model. Because of the head may be influenced by the bracket, the self-balanced NHP was not achievable. Moreover, the subject's eyesight will be blocked by the component of the FaceScan machine, so it was impossible to install a mirror directly in front of the subject with the proper size and location. In other words, it was not possible to acquire NHP with the aid of a mirror. In this study, eNHP was based on the subject's proprioception and the researcher's subjective assessment assisted by orthogonal lasers and was different from the definition of NHP in previous studies.^{27,41}

CONCLUSIONS

This in vivo study proposed a standardized procedure to acquire highly reproducible 3D facial models through structured light scanning. The 6 facial regions, including forehead, nose, paranasal area, upper lip, lower lip and chin, and cheek area, demonstrate satisfying interclass reproducibility. The 95% CI of RMS provides a reference for facial volume change assessment.

AUTHOR CREDIT STATEMENT

Xin-wen Wang contributed to conceptualization, methodology, formal analysis, original draft preparation, and visualization; Zi-jin Liu contributed to validation; Jing Diao contributed to validation; Yi-jiao Zhao contributed to software and methodology; and Jiu-hui Jiang contributed to supervision.

ACKNOWLEDGMENTS

The author would like to thank National Laboratory for Digital and Material Technology of Stomatology, Beijing, China, for software support.

REFERENCES

- Altındış S, Toy E, Başçiftçi FA. Effects of different rapid maxillary expansion appliances on facial soft tissues using three-dimensional imaging. *Angle Orthod* 2016;86:590-8.
- Kook MS, Jung S, Park HJ, Oh HK, Ryu SY, Cho JH, et al. A comparison study of different facial soft tissue analysis methods. *J Craniomaxillofac Surg* 2014;42:648-56.
- Zhao YJ, Xiong YX, Yang HF, Wang Y. [Evaluation of measurement accuracy of three facial scanners based on different scanning principles]. *Beijing Da Xue Xue Bao Yi Xue Ban* 2014;46:76-80. Chinese.
- Dindaroğlu F, Duran GS, Görgülü S. Effects of rapid maxillary expansion on facial soft tissues: deviation analysis on three-dimensional images. *J Orol Orthop* 2016;77:242-50.
- Dolci C, Pucciarelli V, Gibelli DM, Codari M, Marelli S, Trifirò G, et al. The face in Marfan syndrome: a 3D quantitative approach for a better definition of dysmorphic features. *Clin Anat* 2018;31:380-6.
- Ferrario VF, Sforza C, Schmitz JH, Santoro F. Three-dimensional facial morphometric assessment of soft tissue changes after orthognathic surgery. *Oral Surg Oral Med Oral Pathol Oral Radiol Endod* 1999;88:549-56.
- Shi Y, Shang H, Tian L, Bai S, Liu W, Liu Y. [Three-dimensional study of facial soft tissue changes in patients with skeletal Class III malocclusion before and after orthognathic surgery]. *Zhongguo Xiu Fu Chong Jian Wai Ke Za Zhi* 2018;32:612-6. Chinese.
- Wei Y, Chen G, Han B, Hu XY, Zhang HP, Deng XL. [Three-dimensional imaging for quantitative evaluation of facial profile of edentulous patients before and after complete dentures restoration]. *Beijing Da Xue Xue Bao Yi Xue Ban* 2014;46:100-3. Chinese.
- Liu Y, Kau CH, Talbert L, Pan F. Three-dimensional analysis of facial morphology. *J Craniofac Surg* 2014;25:1890-4.
- Clark SL, Teichgraber JF, Fleshman RG, Shaw JD, Chavarría C, Kau CH, et al. Long-term treatment outcome of presurgical nasalveolar molding in patients with unilateral cleft lip and palate. *J Craniofac Surg* 2011;22:333-6.
- Ye H, Lv L, Liu Y, Liu Y, Zhou Y. Evaluation of the accuracy, reliability, and reproducibility of two different 3D face-scanning systems. *Int J Prosthodont* 2016;29:213-8.
- Ma L, Xu T, Lin J. Validation of a three-dimensional facial scanning system based on structured light techniques. *Comput Methods Programs Biomed* 2009;94:290-8.
- Secher JJ, Darvann TA, Pinholt EM. Accuracy and reproducibility of the DAVID SLS-2 scanner in three-dimensional facial imaging. *J Craniomaxillofac Surg* 2017;45:1662-70.
- Gibelli D, Dolci C, Cappella A, Sforza C. Reliability of optical devices for three-dimensional facial anatomy description: a systematic review and meta-analysis. *Int J Oral Maxillofac Surg* 2020;49:1092-106.
- Bjorn H, Lundqvist C, Hjelmstrom P. A photogrammetric method of measuring the volume of facial swellings. *J Dent Res* 1954;33:295-308.
- Peng JX, Jiang JH, Zhao YJ, Wang Y, Li Z, Wang NN, et al. [Preliminary evaluation on 3-dimension changes of facial soft tissue with structure light scanning technique before and after orthognathic surgery of Class III deformities]. *Beijing Da Xue Xue Bao Yi Xue Ban* 2015;47:98-103. Chinese.
- Tang ZL, Wang X, Yi B. [Reverse-engineering-based quantitative three-dimensional measurement of facial swelling after administration of Yunnan Baiyao following orthognathic surgery]. *Zhonghua Yi Xue Za Zhi* 2008;88:2482-6. Chinese.
- van Loon B, van Heerbeek N, Bierenbroodspot F, Verhamme L, Xi T, de Koning MJ, et al. Three-dimensional changes in nose and upper lip volume after orthognathic surgery. *Int J Oral Maxillofac Surg* 2015;44:83-9.
- Kau CH, Cronin A, Durning P, Zhurov AI, Sandham A, Richmond S. A new method for the 3D measurement of postoperative swelling following orthognathic surgery. *Orthod Craniofac Res* 2006;9:31-7.
- Mailey B, Baker JL, Hosseini A, Collins J, Suliman A, Wallace AM, et al. Evaluation of facial volume changes after rejuvenation surgery using a 3-dimensional camera. *Aesthet Surg J* 2016;36:379-87.
- Pinheiro M, Ma X, Fagan MJ, McIntyre GT, Lin P, Sivamurthy G, et al. A 3D cephalometric protocol for the accurate quantification of the craniofacial symmetry and facial growth. *J Biol Eng* 2019;13:42.
- Kau CH, Richmond S. Three-dimensional analysis of facial morphology surface changes in untreated children from 12 to 14 years of age. *Am J Orthod Dentofacial Orthop* 2008;134:751-60.
- Hermans DJ, Maal TJ, Bergé SJ, van der Vleuten CJ. Three-dimensional stereophotogrammetry: a novel method in volumetric measurement of infantile hemangioma. *Pediatr Dermatol* 2014;31:118-22.
- Rizzo MI, Zadeh R, Bucci D, Palmieri A, Monarca C, Staderini E, et al. Volumetric analysis of cleft lip deformity using 3D stereophotogrammetry. *Ann Ital Chir* 2019;90:281-6.
- Rawlani R, Qureshi H, Rawlani V, Turin SY, Mustoe TA. Volumetric changes of the mid and lower face with animation and the standardization of three-dimensional facial imaging. *Plast Reconstr Surg* 2019;143:76-85.
- Seager DC, Kau CH, English JD, Tawfik W, Bussa HI, Ahmed Ael Y. Facial morphologies of an adult Egyptian population and an adult Houstonian white population compared using 3D imaging. *Angle Orthod* 2009;79:991-9.
- Cassi D, De Biase C, Tonni I, Gandolfini M, Di Blasio A, Piacino MG. Natural position of the head: review of two-dimensional and three-dimensional methods of recording. *Br J Oral Maxillofac Surg* 2016;54:233-40.
- He Y, Liang B, Yang J, Li S, He J. An iterative closest points algorithm for registration of 3D laser scanner point clouds with geometric features. *Sensors (Basel)* 2017;17:1862.
- Marlière DA, Demétrio MS, Schmitt AR, Lovisi CB, Asprino L, Chaves-Netto HD. Accuracy between virtual surgical planning and actual outcomes in orthognathic surgery by iterative closest point algorithm and color maps: a retrospective cohort study. *Med Oral Patol Oral Cir Bucal* 2019;24:e243-53.
- Kau CH, Richmond S, Zhurov AI, Knox J, Chestnutt I, Hartles F, et al. Reliability of measuring facial morphology with a 3-dimensional laser scanning system. *Am J Orthod Dentofacial Orthop* 2005;128:424-30.
- Maués CPR, Casagrande MVS, Almeida RCC, Almeida MAO, Carvalho FAR. Three-dimensional surface models of the facial soft tissues acquired with a low-cost scanner. *Int J Oral Maxillofac Surg* 2018;47:1219-25.
- Gibelli D, Pucciarelli V, Caplova Z, Cappella A, Dolci C, Cattaneo C, et al. Validation of a low-cost laser scanner device for the assessment of three-dimensional facial anatomy in living subjects. *J Craniomaxillofac Surg* 2018;46:1493-9.

33. Camison L, Bykowski M, Lee WW, Carlson JC, Roosenboom J, Goldstein JA, et al. Validation of the Vectra H1 portable three-dimensional photogrammetry system for facial imaging. *Int J Oral Maxillofac Surg* 2018;47:403-10.
34. Gibelli D, Pucciarelli V, Cappella A, Dolci C, Sforza C. Are portable stereophotogrammetric devices reliable in facial imaging? A validation study of VECTRA H1 device. *J Oral Maxillofac Surg* 2018;76:1772-84.
35. Zhao YJ, Xiong YX, Wang Y. Three-dimensional accuracy of facial scan for facial deformities in clinics: a new evaluation method for facial scanner accuracy. *PLoS One* 2017;12:e0169402.
36. Knoop PG, Beaumont CA, Borghi A, Rodriguez-Florez N, Breakey RW, Rodgers W, et al. Comparison of three-dimensional scanner systems for craniomaxillofacial imaging. *J Plast Reconstr Aesthet Surg* 2017;70:441-9.
37. Li H, Cao T, Zhou H, Hou Y. Lip position analysis of young women with different skeletal patterns during posed smiling using 3-dimensional stereophotogrammetry. *Am J Orthod Dentofacial Orthop* 2019;155:64-70.
38. Tingey EM, Buschang PH, Throckmorton GS. Mandibular rest position: a reliable position influenced by head support and body posture. *Am J Orthod Dentofacial Orthop* 2001;120:614-22.
39. Miles TS. Postural control of the human mandible. *Arch Oral Biol* 2007;52:347-52.
40. Watarai Y, Mizuhashi F, Sato T, Koide K. Highly producible method for determination of occlusal vertical dimension: relationship between measurement of lip contact position with the closed mouth and area of upper prolabium. *J Prosthodont Res* 2018;62:485-9.
41. Tian K, Li Q, Wang X, Liu X, Wang X, Li Z. Reproducibility of natural head position in normal Chinese people. *Am J Orthod Dentofacial Orthop* 2015;148:503-10.
42. Caple J, Stephan CN. A standardized nomenclature for craniofacial and facial anthropometry. *Int J Legal Med* 2016;130:863-79.